JOURNAL OF MATERIALS SCIENCE 15 (1980) 1097–1103

Mechanical properties characterization of the broken-lamellar eutectic composite Cd-Ge

M. SAHOO*, G. W. DELAMORE†, R. W. SMITH
Department of Metallurgical Engineering, Queen's University, Kingston, Ontario, Canada K7L 3N6

The tensile and compressive properties of the unidirectionally solidified Cd–Ge eutectic have been examined. With increasing growth rate the broken-lamellar Ge–rich phase becomes increasingly fibrous. This morphological change was accompanied by a marked increase in tensile properties, similar to the changes observed for both Zn–Ge and Al–Si. However, a less dramatic increase in compressive properties took place. The presence of Cd dendrites did not reduce the UCS (ultimate compressive strength) as has been reported for Cd–Zn and Sb–Ge. Large matrix constraints arise in this eutectic even though the weight fraction of the Ge phase is only 2%.

1. Introduction

It has been shown that by consideration of the entropy of solution (Δs) and the volume fraction (V_f) of the minor phase, anomalous (faceted/non-faceted) eutectics can be further subdivided into four distinct structural types; namely, "broken-lamellar", "irregular", "complex-regular" and "quasi-regular" [1]. The mechanical properties of a number of "irregular eutectics" for which $V_f = 6$ to 18% have already been examined [2–5] as have those of various regular eutectics [6, 7]. In order to produce a general mechanical properties characterization of eutectics, it was of interest to examine the mechanical properties of anomalous eutectics exhibiting the broken-lamellar microstructure. Of these, the Cd–Ge eutectic appeared particularly suitable. This eutectic contains 2 wt% of the faceting Ge phase in the Cd matrix. Thus it is a typical metal/non-metal eutectic combination. Of the various possible metal/non-metal eutectic alloys in which the minor phase is virtually the pure non-metallic element, the structure and mechanical properties of the Ag–Ge [8], Al–Si [2, 3] and Zn–Ge [4] alloys have already been examined in detail. However, no information is available on the structure and mechanical behaviour of the Cd–Ge eutectic.

Thus, the objectives of the present investigation were to characterize the tensile and compression properties of the Cd–Ge eutectic over a wide range of growth conditions, as was done with the Al–Si and Zn–Ge eutectics. In addition, this eutectic contains only 2 vol% of the faceting Ge phase in the Cd matrix. Thus the relative separation of regions of the reinforcing minor phase will be large and so any constraints offered by the matrix might be expected to be insignificant. Hence, it was presumed that the UTS (ultimate tensile strength) of the composite might be obtained directly from the rule of mixtures by substituting the bulk properties of both minor phase and matrix.

2. Experimental details

Cd–Ge eutectic alloys with a nominal germanium content of 1.9 wt% Ge were prepared from 99.9999 wt% Cd and 99.999 wt% Ge. Weighed amounts of Cd and Ge were encapsulated in argon-filled 12 mm i.d. Pyrex tubes, heated in a gas flame to melt the constituents and shaken vigorously

*Present address: CANMET/EMR 568 Booth Street, Ottawa, Ontario, Canada.
†Present address: Department of Metallurgy, University of Woolongong, New South Wales, Australia.

0022–2461/80/051097–07$02.70/0

to encourage complete mixing. The solidified rods were swaged to 5 mm diameter to promote homogeneity. The rods were then sealed into argon-filled 6 mm i.d. Pyrex tubes for melting and directionally solidifying by lowering the tube through a tube furnace set at 360° C into a water jacket located 15 mm below the furnace. This provided a temperature gradient (G) of 7° C mm^{-1} at a growth rate (R) of 50 mm h^{-1}.

The first and last 3 cm of each alloy were rejected and the tensile and compressive testing specimens were cut from the remainder. Longitudinal and transverse sections were prepared for metallographic examination.

Specimens for tensile testing were machined in a jeweller's lathe to produce a reduced diameter of 3.9 mm. Compressive specimens, 12.0 mm long and 5.0 mm diameter, were carefully polished to produce parallel faces and then etched to remove any worked layer. All tensile and compressive tests were performed at ambient temperatures (~ 25° C) with the stress axis parallel to the growth axis, using an Instron testing machine at a cross-head speed of ~ 0.13 mm min^{-1}. In the case of tensile tests, a 25.4 mm Instron extensometer was used to measure specimen elongations.

Metallographic specimens were cold-mounted, polished in the conventional manner and finally etched in a solution of 320 g CrO_3, 20 g Na_2SO_4, made to 1000 ml in water.

The orientation of the matrix was examined using X-ray pole-figure techniques.

3. Results and discussion

3.1. Microstructure

Representative optical micrographs of transverse sections through Cd–1.9 wt % Ge eutectic alloys directionally solidified at various growth rates are illustrated in Figs. 1 to 6. It is evident from Fig. 1 that the Cd–Ge eutectic does indeed possess a broken-lamellar morphology. The interlamellar spacings (λ) measured in transverse sections were found to be of the order of 35 μm, i.e., very large as compared with regular eutectics grown under similar conditions. A longitudinal section of the quenched growth-front corresponding to the specimen Fig. 1a is shown in Fig. 1b. This optical micrograph suggests that the growth front is non-isothermal and is similar to that observed in the Al–Si system by Day and Hellawell [9] who showed that the silicon grew in a preferred ⟨1 0 0⟩.

With further increases in growth rate, the Ge phase became gradually finer and the interlamellar spacing decreased. At growth rates greater than 150 mm h^{-1} the eutectic microstructure was characterized by the presence of Cd dendrites in

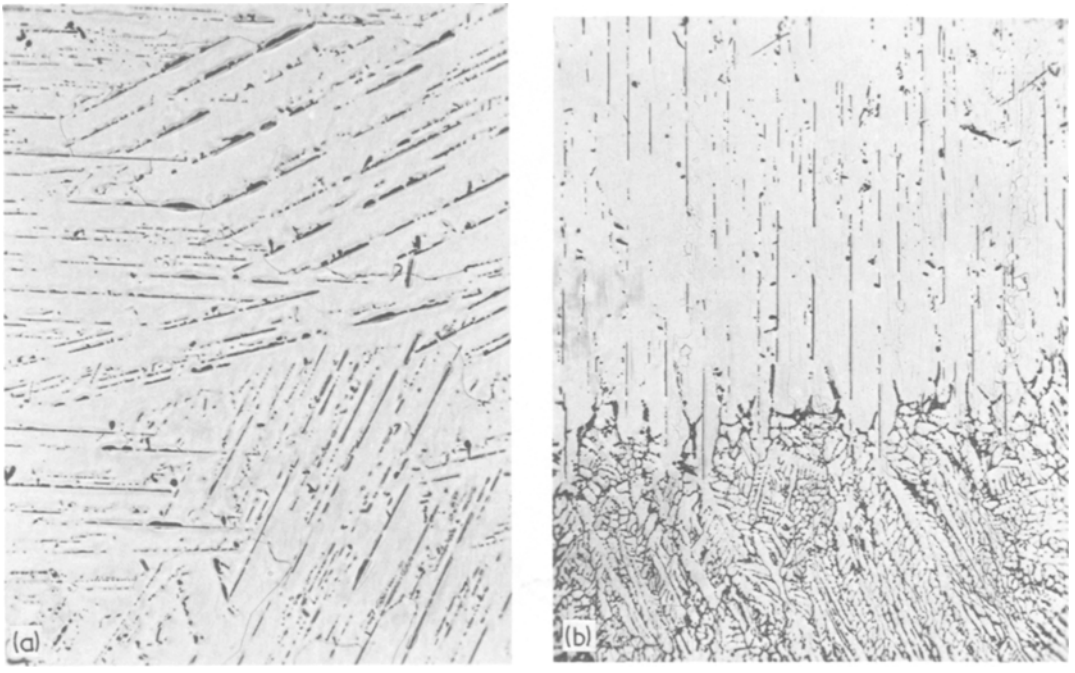

Figure 1 Optical micrographs of directionally solidified Cd–Ge eutectic showing the broken-lamellar Ge morphology at a growth rate of 17 mm h^{-1}. (a) Transverse section (× 75). (b) Longitudinal section of quenched interface (× 56.25).

Figure 2 Optical micrograph of the directionally solidified Cd–Ge eutectic composite showing the broken-lamellar Ge morphology at a growth rate of 40 mm h^{-1} (× 150).

addition to the fine broken-lamellar form of Ge (Fig. 3). At growth rates greater than 1000 mm h^{-1}, the microstructure changed to a fibrous form (Fig. 5).

The grain diameter of the columnar Cd matrix was of the order of 1 to 2 mm.

The presence of Cd dendrites at a growth rate of 150 mm h^{-1} (Fig. 3a) corresponds to the onset of constitutional undercooling. At the solid–liquid interface, the temperature gradients in the solid and liquid, G_s and G_l are related by

$$K_s G_s = K_l G_l + L\rho R$$

where K_s and K_l are the thermal conductivities in the solid and liquid respectively, L is the latent heat of fusion, ρ is the density and R is the growth velocity. Since the distance between the tube furnace and the water jacket was fixed for all growth rates, with increasing growth rates the interface moves closer to the water jacket. Hence, G_l decreases with increasing growth rate to permit constitutional undercooling to arise. In the present case, the G_l was found to be 7° C mm^{-1} for a growth rate of 40 mm h^{-1}. However, at a growth rate of 150 mm h^{-1}, G_l decreased to 4° C mm^{-1}. It was also observed that by increasing G_l to $\simeq$ 18° C mm^{-1} constitutional supercooling could be avoided since Cd primaries were not observed until the growth rate exceeded 280 mm h^{-1}.

Figure 3 Optical micrographs of directionally solidified Cd–Ge eutectic showing the presence of Cd primaries together with the broken-lamellar Ge morphology at a growth rate of 150 mm h^{-1}. (a) Transverse section (× 75); and (b) longitudinal section (× 75).

Figure 4 Optical micrograph of the directionally solidified Cd–Ge showing the broken-lamellar Ge morphology and Cd primaries at a growth rate of 280 mm h^{-1} (× 150).

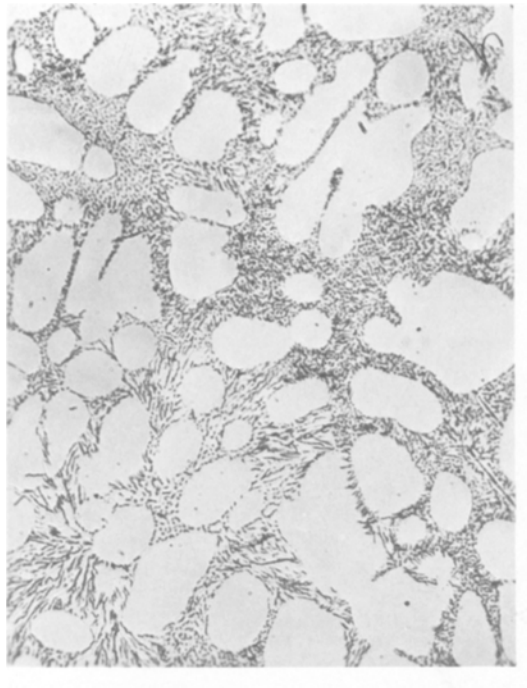

Figure 5 Optical micrograph of the directionally solidified Cd–Ge eutectic showing the fibrous Ge morphology at a growth rate of 1150 mm h^{-1} (× 375).

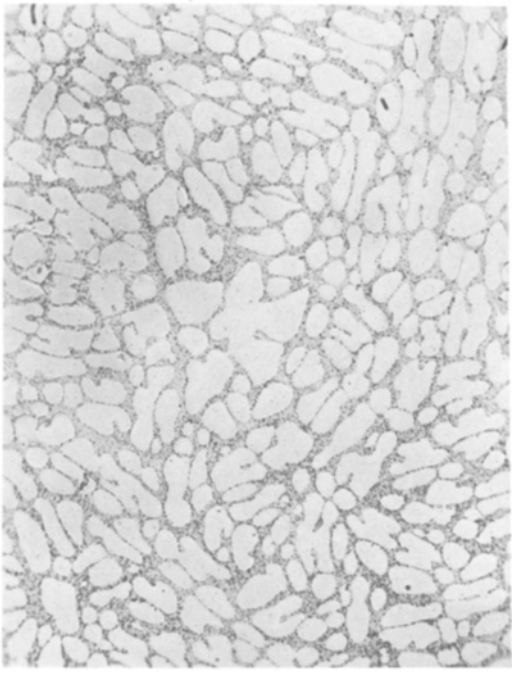

Figure 6 Optical micrograph of the directionally solidified Cd–Ge eutectic showing the fibrous Ge morphology at a growth rate of 5000 mm h^{-1} (× 375).

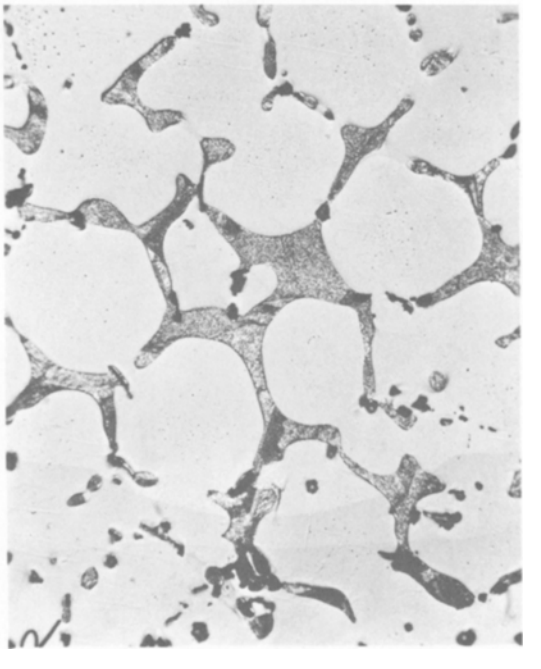

Figure 7 Optical micrograph of the sodium-modified Cd–Ge eutectic. Polarized light (× 150).

It is well known that both Si and Ge are sensitive to additions of Na. Thus additions of about 0.05 wt% elemental sodium to the melt prior to freezing modified the morphology of the broken lamellar Ge to a fibrous form (Fig. 7). Thermal analysis of the unmodified and sodium-modified Cd–Ge eutectic alloys showed that, in common with Al–Si and Zn–Ge eutectic alloys, the addition of sodium displaced the eutectic plateau to lower temperatures during continuous cooling. In the present case, a supercooling of 7° C was observed when 0.05% Na was added to the melt. However, the eutectic melting temperature was unchanged. In unmodified samples, the eutectic freezing and melting temperatures were essentially the same.

3.2. Mechanical properties

Table I summarizes the room temperature tensile and compression properties of the Cd–Ge eutectic alloys. Typical room temperature stress–strain curves are shown in Fig. 9. These curves are drawn only up to the UTS of the eutectic since failure did not occur at the UTS. The total strain for failure varies between 6 to 16%. Thus the Cd–Ge eutectic can be classified as a ductile composite.

Table I shows that at low growth rates ($\leqslant 40\,mm\,h^{-1}$), the eutectic has a UTS of about $36\,N\,mm^{-2}$. Further increases in growth rate produced a finer eutectic structure and corresponding increases in the UTS. At the highest growth rate ($5000\,mm\,h^{-1}$), the UTS of the eutectic reached a value of $81\,N\,mm^{-2}$ and corresponds to more than a two-fold increase in strength due to modification of the microstructure. A similar two-fold increase was observed for Al–Si [2] and Zn–Ge [4] eutectic alloys. It is interesting to note that the presence of the Cd primaries in specimens grown faster than $150\,mm\,h^{-1}$ did not adversely affect the tensile properties.

The increases in compressive strength were not as dramatic. The UCS of the eutectic at the lowest growth rate was about $75\,N\,mm^{-2}$. With increases in growth rate, the UCS increased to about $120\,N\,mm^{-2}$ at a growth rate of $280\,mm\,h^{-1}$. At extremely fast growth rates there was a small decrease in UCS. This is similar to the observation made in case of Zn–Ge alloys.

TABLE I Room temperature mechanical properties of directionally solidified Cd–Ge eutectics

Growth rate ($mm\,h^{-1}$)	Tension			Compression			Microstructure
	0.2% yield strength ($N\,mm^{-2}$)	UTS ($N\,mm^{-2}$)	Uniform elongation (%)	0.2% yield strength ($N\,mm^{-2}$)	UCS ($N\,mm^{-2}$)	Uniform elongation (%)	
5.8	24	39	4.0	66	72	2.1	Coarse broken-lamellar
				67	79	1.5	
17	20	34	7.3	69	83	1.4	Fine broken-lamellar
40	21	37	5.8	69	90	5.7	Fine broken-lamellar
				67	94	5.1	
150	43	54	4.7	94	115	3.2	Fine broken-lamellar plus Cd-primaries
176	52	61	1.5	76	107	12.5	Fine broken-lamellar plus Cd-primaries
				71	105	12.5	
176 (grown with high temperature gradient)				76			Fine broken-lamellar
				80			
280	44	65	8.0	105	121	2.3	Fine broken-lamellar plus Cd-primaries
				102	121	3.3	
				99	118	3.0	
1150	53	61	4.0	76	99	6.3	Fibrous plus Cd-primaries
5000	75	81	0.7	77	114	7.5	Fibrous plus Cd-primaries
				93	114	3.8	

Table I shows that for any growth rate the compressive yield and ultimate strengths are higher than the respective tensile properties. This is similar to the differences observed in other eutectic systems [2–6, 10]. This form of response is usually attributed to the residual stresses due to differences in the thermal expansion coefficients of the two phases. The thermal expansion coefficient for Ge (α_{Ge}) is $6 \times 10^{-6\circ} C^{-1}$ [11], whereas α_{Cd} perpendicular to the hexagonal axis is $42 \times 10^{-6\circ} K^{-1}$ [12]. Since $\alpha_{Cd} > \alpha_{Ge}$ the residual stresses developed cooling from the eutectic temperature are tensile in the Cd matrix and compressive in the Ge phase. Thus the matrix will yield at a lower stress level in tension than in compression.

It may be noted that when the Cd–Ge eutectic was grown in a large temperature gradient to suppress the formation of Cd primaries (see $176\,mm\,h^{-1}$), the compressive strength remained unchanged.

It is interesting to compare the above behaviour with that of other systems with a small V_f value. In Cd–Zn alloys [6], whilst the presence of ductile primaries did little to change the UTS values, a two-fold decrease in UCS was noted. Again, in the Sb–Ge system, which was not tested in tension due to its brittle nature [5], the UCS was halved when brittle, antimony dendrites were present.

The reason for this is not clear since such behaviour is not expected following consideration of the application of the rule of mixtures to the Cd–Ge system. Using the rule of mixtures [10], and a value of $1300\,N\,mm^{-2}$ for the germanium fibres [13] and $35\,N\,mm^{-2}$ for the cadmium matrix [14], the tensile strength of the composite is estimated to be about $60\,N\,mm^{-2}$. This closely parallels the values obtained for Zn–Ge, namely an estimated value of $160\,N\,mm^{-2}$ and measure value of $200\,N\,mm^{-2}$. Thus even though the volume fraction of the germanium reinforcing phase in Cd–Ge is only one-third that of the germanium in Zn–Ge, matrix constraints of similar magnitude appear to be present. However, the replacement of regions of the fibre-strengthened composite by germanium-free cadmium dendrites might have been expected to decrease the compressive strength.

Figure 8 Optical micrograph of longitudinal section near fraction surface of the Cd–Ge eutectic alloy showing deformation twins, grown at a growth rate of $17\,mm\,h^{-1}$.

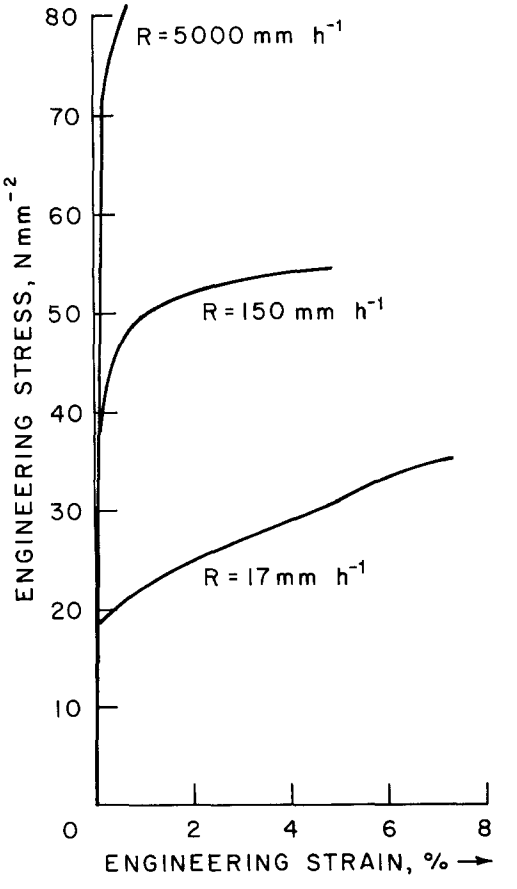

Figure 9 Room temperature engineering tensile stress–strain curves for Cd–Ge eutectic alloys directionally solidified at various rates.

Metallographic examination of longitudinal sections through the fractured surface of specimens tested in tension showed deformation twins (Fig. 8). In addition, the load–elongation curves gave a saw-tooth appearance characteristic of twin-controlled deformation. This is similar to the observation made in case of the Cd–Zn eutectic.

In compression, the specimens grown at lower rates showed the shear mode buckling described for Zn–Ge eutectic specimens [4]. The shear occurred at approximately 45° to the axis of compression and, since the growth axis of low melting point hexagonal metals at low growth rates is $\langle 0\,0\,0\,1 \rangle$ [15], the slip plane is $\{1\,1\,2\,\bar{2}\}$ throughout the section. No such buckling was observed in specimens grown at 3600 mm h^{-1}. This is presumably due to the structure being cellular, fine-grained, with the (0 0 0 1) of local regions being parallel to the growth direction. As such the matrix is more able to provide appropriate mechanical restraint on the phase containing the maximum resolved shear stress and so render massive shear impossible.

4. Conclusions

(1) Cd–Ge is normally a broken-lamellar eutectic, becoming fibrous at large growth rates and on the addition of sodium.

(2) As the growth rate increases, tensile properties increase in a marked manner, similar to that of both Zn–Ge and Al–Si. However, a less dramatic increase occurs in compressive properties.

(3) The presence of primary cadmium dendrites does not reduce the UCS as has been reported for Cd–Zn and Sb–Ge eutectic alloys.

(4) Application of the rule of mixtures suggests that, providing the critical volume fraction of reinforcing phase is exceeded, matrix constraints appear and so the observed mechanical strength exceeds the calculated value.

Acknowledgements

The authors wish to acknowledge the financial support of the National Science and Engineering Research Council of Canada and the Queen's Research Award Programme.

References

1. M. N. CROKER, R. S. FIDLER and R. W. SMITH, *Proc. Roy. Soc.* **A335** (1973) 15.
2. M. SAHOO and R. W. SMITH, *Met. Sci.* 9 (1975) 217.
3. *Idem, Canad. Met. Q.* **15** (1976) 1.
4. *Idem, J. Mater. Sci.* **11** (1976) 1125.
5. M. SAHOO, D. BARAGER and R. W. SMITH, *ibid* **13** (1978) 1565.
6. M. SAHOO, R. A. PORTER and R. W. SMITH, *ibid* **11** (1976) 1680.
7. M. SAHOO and R. W. SMITH, *ibid* **13** (1978) 283.
8. W. R. KRUMMHEUER and H. ALEXANDER, *ibid* 9 (1974) 229.
9. M. R. DAY and A. HELLAWELL, *Proc. Roy. Soc.* **A305** (1968) 473.
10. H. BIBRING, "Proceedings of the Conference on *in situ* Composites", Vol. II (National Academy of Science, Washington D.C. 1972) p. 1.
11. C. J. SMITHELS, "Metals Reference Book", 4th edn. (Butterworth, London, 1967).
12. N. MADAIAH and G. M. GRAHAM, *Canad. J. Phys.* **42** (1964) 246.
13. G. L. PEARSON, W. T. READ and W. L. FIELDMAN, *Acta Met.* **5** (1967) 181.
14. N. R. RISEBROUGH, Ph.D. thesis, University of British Columbia, Canada (1964).
15. A. HELLAWELL and P. M. HERBERT, *Proc. Roy. Soc. (London)* **A269** (1962) 560.

Received 19 July and accepted 27 September 1979.